RESEARCH ARTICLE SUMMARY

STEM CELLS

Stem cells expand potency and alter tissue fitness by accumulating diverse epigenetic memories

Kevin Andrew Uy Gonzales, Lisa Polak, Irina Matos, Matthew T. Tierney, Anita Gola, Ellen Wong, Nicole R. Infarinato, Maria Nikolova, Shijing Luo, Siqi Liu, Jesse S. S. Novak, Kenneth Lay, Hilda Amalia Pasolli, Elaine Fuchs*

INTRODUCTION: Tissue stem cells respond to and integrate environmental cues to determine their fate and function. Injury induces radical changes in the microenvironment that trigger stem cells to undergo a multitude of choreographed experiences that include departing their original niche, migrating into a wound bed, overcoming inflammation, generating tissue de novo, and taking up residence at the new site. Wounds can also induce plasticity, mobilizing stem cells to repair related but different tissues. It remains unclear whether stem cells accumulate and retain memories of these spatially and temporally defined experiences in injury repair, and if so, how this happens and what the consequences are.

RATIONALE: Within the hair follicle (HF), bulge stem cells (HFSCs) normally only make hair, but they become repurposed when a wound damages the overlying skin tissue. Using lineage tracing, we monitored HFSCs as they temporally progress through this journey of wound repair and stem cell plasticity. After leaving their niche and regenerating missing tissue, they can remain long-term in the de novo epidermis and thereafter maintain the skin's barrier. By exploring transcriptome and epigenome dynamics and interrogating the behavior of these immigrant stem cells in their new niche, we learned that these stem cells accumulate discrete epigenetic memories of their past experiences, each of which affects overall tissue function in different ways.

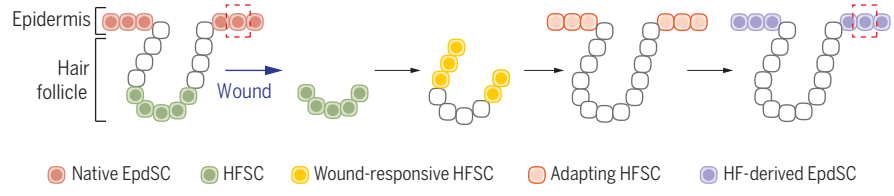

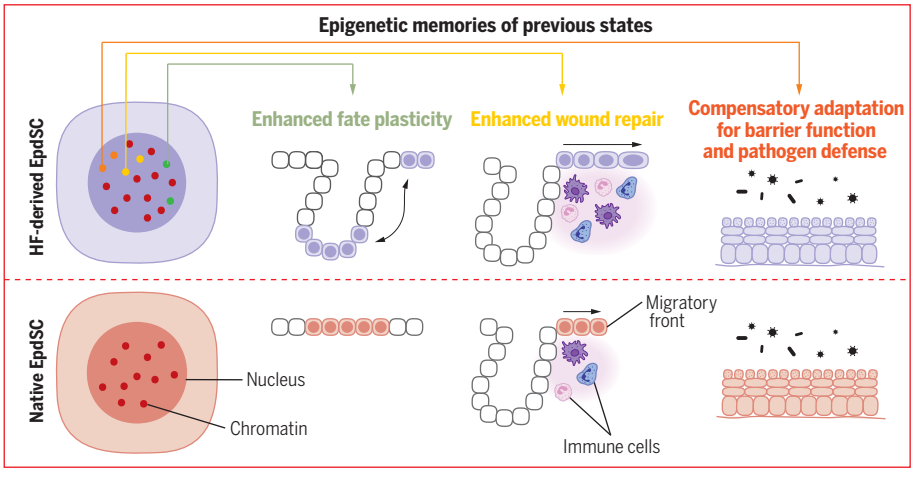

Stem cells accumulate epigenetic memories of their past experiences. As hair follicle stem cells mobilize to repair wounded skin epidermis and take up residence as epidermal stem cells, they temporally change chromatin states. Each environmental encounter leaves a discrete long-lasting epigenetic memory, enabling these immigrant stem cells to perform their new tasks while also heightening future responses to injury, inflammation, and hair regeneration.

RESULTS: By denuding the epidermis, we coaxed underlying HFSCs to be the primary responders to re-epithelialization. This creates a long-term, self-renewing epidermis that is largely HF-derived. The fate-changed epidermal stem cells (EpdSCs) were indistinguishable from native unwounded EpdSCs in homeostatic function and transcriptome. However, assay for transposase-accessible chromatin using sequencing (ATAC-seq) revealed many loci with increased accessibility. Open chromatin domains distinguishing HF-derived from native EpdSCs came in three forms: (i) domains that increased accessibility only during adaptation to the new epidermal niche (compensatory adaptation), (ii) domains that opened during the wound response (memory of wound), and (iii) domains that were already open in quiescent HFSCs (memory of niche origin). Each enduring epigenetic memory had its own consequence. Compensatory adaptation domains enabled key differentiation and immune defense transcripts necessary for maintaining the skin's barrier to be expressed at native levels. Wound memory domains primed genes involved in inflammation, cytoskeletal reorganization, and migration to be robustly induced upon secondary wounds, thus accelerating healing. Memory of niche origin domains were associated with genes involved in HFSC fate and WNT signaling, imparting plasticity to revert to the HF fate given the right environmental cues. Finally, these memories, although cumulative, were distinct, separable, and dependent on past experiences. Thus, EpdSCs that repaired epidermal injuries exhibited a wound memory but lacked memories of HF niche origin and epidermal compensatory adaptation.

CONCLUSION: The concept of epigenetic memory was first reported in inflammatory contexts. Here, we found that additional memories are acquired and maintained in the chromatin of tissue stem cells, which suggests that stem cells can store epigenetic memories from different experiences they encounter. By influencing a stem cell's responses to future assaults, such memories can have an impact on long-term tissue fitness in either beneficial or detrimental ways, depending on context. ■

The list of author affiliations is available in the full article online.
*Corresponding author. Email: fuchslb@rockefeller.edu
Cite this article as K. A. U. Gonzales *et al.*, *Science* **374**, eabh2444 (2021). DOI: 10.1126/science.abh2444

READ THE FULL ARTICLE AT
https://doi.org/10.1126/science.abh2444

RESEARCH ARTICLE

STEM CELLS

Stem cells expand potency and alter tissue fitness by accumulating diverse epigenetic memories

Kevin Andrew Uy Gonzales[1], Lisa Polak[1], Irina Matos[1,2], Matthew T. Tierney[1], Anita Gola[1], Ellen Wong[1], Nicole R. Infarinato[1], Maria Nikolova[1], Shijing Luo[3], Siqi Liu[1], Jesse S. S. Novak[1], Kenneth Lay[4], Hilda Amalia Pasolli[5], Elaine Fuchs[1]*

Immune and tissue stem cells retain an epigenetic memory of inflammation that intensifies sensitivity to future encounters. We investigated whether and to what consequence stem cells possess and accumulate memories of diverse experiences. Monitoring a choreographed response to wounds, we found that as hair follicle stem cells leave their niche, migrate to repair damaged epidermis, and take up long-term foreign residence there, they accumulate long-lasting epigenetic memories of each experience, culminating in post-repair epigenetic adaptations that sustain the epidermal transcriptional program and surface barrier. Each memory is distinct, separable, and has its own physiological impact, collectively endowing these stem cells with heightened regenerative ability to heal wounds and broadening their tissue-regenerating tasks relative to their naïve counterparts.

Specialized environments called "niches" enable adult stem cells (SCs) to balance self-renewal with differentiation to maintain tissue homeostasis (*1*–*3*). Fate determination depends on the intrinsic abilities of resident SCs to integrate and respond appropriately to inductive environmental cues (*4*–*9*). Tissue injury unleashes the lineage option constraints normally imposed by distinct niches, and it mobilizes nearby closely related SCs to trigger a transient state of plasticity as they migrate into and repair the wound. Plasticity is resolved when the SC either returns to its original niche and duties, or alternatively, takes up residence within the repaired tissue (*1*, *10*). Once a SC adopts a new fate and enters a new niche, however, it remains unclear how long this repurposed SC will survive in its new tissue and to what extent it behaves similarly to its native counterparts in performing its new tasks. Moreover, during wound repair, these immigrant SCs will have also encountered a multitude of choreographed experiences that include departing their original niche, migrating into a wound bed, overcoming inflammation, generating a different tissue de novo, and participating in a different lineage program. Do stem cells accumulate and retain memories of these spatially and temporally defined events in injury repair, and if so, how and to what consequence?

[1]Robin Chemers Neustein Laboratory of Mammalian Development and Cell Biology, Howard Hughes Medical Institute, The Rockefeller University, New York, NY 10065, USA. [2]Immunology Discovery, Genentech Inc., South San Francisco, CA 94080, USA. [3]Jones Day Intellectual Property Law Firm, New York, NY 10281, USA. [4]Laboratory of Human Genetics and Therapeutics, Institute of Medical Biology, A*STAR, Singapore 138648, Singapore. [5]Electron Microscopy Resource Center, The Rockefeller University, New York, NY 10065, USA.
*Corresponding author. Email: fuchslb@rockefeller.edu

Although all tissue SCs must respond to and repair local wounds, hair follicle SCs are particularly well suited to explore these questions. Within each hair follicle, the microenvironment of their "bulge" niche normally instructs these SCs to spend prolonged periods in quiescence, until they accumulate sufficient activating cues to synchronously initiate the regeneration of the lower portion of the follicle and grow new hair (*1*). However, upon injury to overlying skin tissue, bulge activity is redirected, mobilizing its SCs to leave the hair follicle, regenerate epidermal tissue de novo, and restore the skin's barrier (*9*, *11*, *12*).

Here, we show that upon wounding, hair follicle–derived epidermal stem cells (HF-derived EpdSCs) can establish long-term residence within the epidermis, where they become transcriptionally indistinguishable from native EpdSCs and are fully functional in fueling the epidermal differentiation program. However, to achieve a normal EpdSC transcriptional program, these foreign residents undergo compensatory adaptation in the form of enhanced chromatin accessibility of the genes encoding key differentiation and immune defense proteins that generate and maintain the skin's barrier. They also accumulate epigenetic memories of experiences that were encountered along their journey. Although these memories are kept dormant during normal homeostasis, they are recalled upon exposure to environmental stimuli that triggered their establishment. Finally, we show that when unleashed, these memories manifest in superior fitness, which includes improved wound repair and hair production.

HFSCs can partake in long-term repair

HFSCs can participate in repairing damaged epidermis, but their relative long-term contributions remain unclear (*9*, *11*, *12*). We therefore challenged different skin SC niches to participate long-term in repairing damaged epidermis. To do so, we introduced shallow, intermediate, or full-thickness (deep) wounds during the prolonged resting phase (telogen) of the hair cycle (fig. S1, A and B). As judged by planar and sagittal immunofluorescence images, shallow wounds removed only epidermis, leaving behind both HF junctional zone (JZ) stem cells (Lrig1$^+$) that rejuvenate the upper HF/sebaceous gland and bulge HFSCs (Krt24$^+$) that fuel hair growth (fig. S1C). By contrast, intermediate wounds removed both epidermis and Lrig1$^+$ JZ in their entirety, exposing the HF bulge with its characteristic hair shaft (green autofluorescence) to the overlying eschar (scab) of day-1 wounds (fig. S1C). With this documentation, we then used lineage-tracing reporter mice to monitor progeny of Krt24$^+$ bulge HFSCs (*Krt19CreER*$^+$*Sox9CreER*$^+$) and Lrig1$^+$ JZ HFSCs (*Sox9CreER*$^+$*Krt19CreER*^{neg}). Figure S2, A to C, shows the lineage tracings used and the fluorescence-activated cell sorting (FACS) strategy to purify and quantify SCs ($\alpha6^+$SCA1$^+$) within re-epithelialized epidermis. These data were normalized to account for CreER targeting efficiency of *Rosa26-fl-stop-fl-YFP* within otherwise transcriptome-homogeneous bulge SCs (*13*).

In agreement with prior studies (*9*, *11*) and underscoring the preferential mobilization of wound-edge EpdSCs in full-thickness wounds (*14*, *15*), most deep wound re-epithelialization came from epidermis (*Sox9*YFP^{neg}) and not HFs (*Sox9*YFP$^+$) (Fig. 1A and fig. S2, D and E). However, in shallow and intermediate wounds, *Sox9*YFP lineage tracings showed >90% contribution, indicating little or no contribution from wound-edge EpdSCs (Fig. 1A and fig. S2F). By contrast, *Krt19*YFP tracings showed that bulge SCs were the major contributors to de novo repaired epidermis in intermediate wounds. There, the percentage of YFP$^+$ HF-derived basal cells within re-epithelialized epidermis was comparable to that within the bulges of unwounded HFs, indicating that intermediate wounds use primarily bulge SCs in repair (fig. S2G). Notably, this percentage of *Krt19YFP* cells in de novo epidermis remained relatively steady even 2 months after wounding, indicating that long-term re-epithelialized epidermis in intermediate wounds was largely derived from bulge HFSCs (Fig. 1A). Together, these findings show that the type of wound affects which SC compartment will predominate in re-epithelialization: deep (EpdSCs), shallow (JZ HFSCs), and intermediate (bulge HFSCs).

HF-derived epidermis is fully functional in homeostasis

At day 60 after wounding, bulge SC–derived (hereafter, HF-derived) epidermis appeared similar to unwounded (native) epidermis in

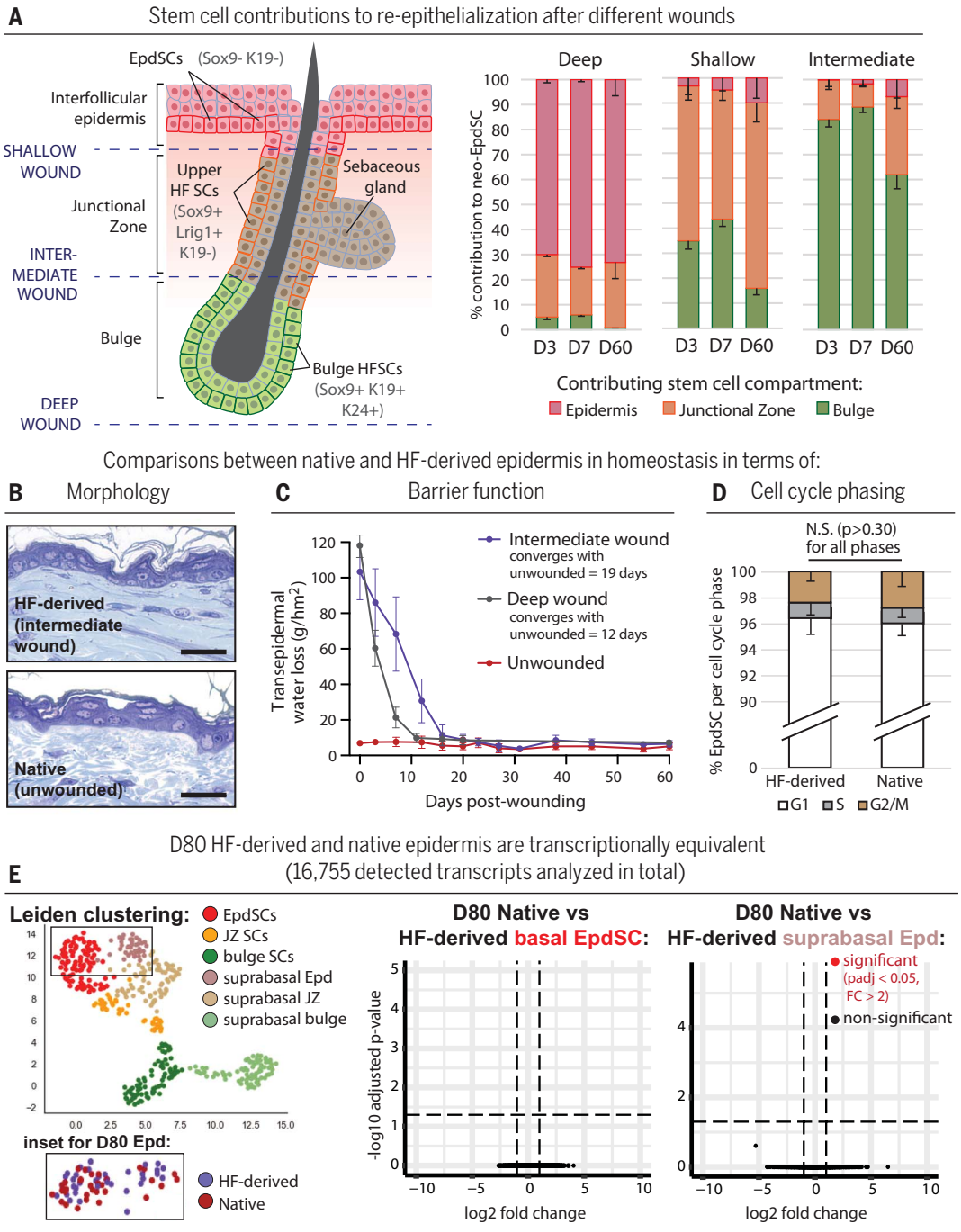

Fig. 1. Hair follicle–derived epidermis is indistinguishable from native epidermis during homeostasis. (**A**) Different niche contributions to re-epithelialization depending on type of wound. Left: SC niches and types of injuries analyzed. Dashed lines indicate which layer of cells are removed in each wounding scenario. Right: Flow cytometry quantifications of stem cell niche contributions to re-epithelialized skin epidermis (Lin^{neg} $\alpha6^{+}$ $Sca1^{+}$ cells; Lin^{neg} = $CD117^{neg}$ $CD45^{neg}$ $CD140a^{neg}$ $CD31^{neg}$) analyzed at days 3, 7, and 60 after wounding (see fig. S2C and supplementary materials). *Sox9CreER* is HF-specific, and its efficient labeling of HFs (~70 to 100%) indicates that repair from shallow and intermediate wounds originates from HFs and not epidermis. *Krt19CreER* is bulge-specific, and when normalized for its low labeling efficiency, it showed little contribution to shallow wounds but strong contribution to intermediate wounds (comparable percentage of *Krt19CreER*-traced EpdSCs in re-epithelialized epidermis and in HFSCs within the bulge). Error bars denote SD of three wounds per time point. (**B**) Toluidine blue–stained semi-thin sections show similar morphologies between day-60 HF-derived and native epidermis. Scale bars, 25 μm. (**C**) Epidermal barrier function analysis. Time-course measurements of trans-epidermal water loss were recorded with a Tewameter. Wound sizes were adjusted such that complete re-epithelialization was achieved in both wound types at day ~6 after wounding. Error bars denote SD for 12 mice. Convergence points were calculated using a one-phase decay model. (**D**) Cell cycle phase distribution based on DNA content in day-70 HF-derived and native EpdSCs (Lin^{neg} $\alpha6^{+}$ $Sca1^{+}$ $CD200^{neg}$), as quantified by flow cytometry. Error bars denote SD for 10 mice. Welch's *t* test was used to calculate *P* value. (**E**) Single-cell transcriptomes of HF-derived EpdSCs are indistinguishable from those of native EpdSCs. Left: UMAP plot of Leiden-clustered transcriptomes from day-0 control, day-80 control, and day-80 intermediate-wounded epithelial cells, with inset indicating the niche origin of day-80 Epd cells. Right: DESeq2 analysis in the EpdSC and suprabasal Epd clusters, showing no differentially expressed genes between native and HF-derived epidermal cells. N.S., not significant.

morphology (Fig. 1B), thickness (fig. S3A), and expression of terminal differentiation–specific markers (fig. S2, F and G). Although trans-epidermal water loss (TEWL) assays indicated a delay in skin barrier restoration for intermediate versus deep wounds, within 19 days after wounding, the eschar (scab) was gone, tight junctions were reestablished, and the skin barrier function of HF-derived epidermis was intact (Fig. 1C and fig. S3B). At this time, proliferation rates and orientations of EpdSC divisions were also comparable between HF-derived and native skins (Fig. 1D and fig. S3, C and D). Thus, in post-repaired homeostatic skin, the epidermis formed from wound-mobilized bulge HFSCs behaved much like native epidermis.

We next performed single-cell RNA sequencing (scRNA-seq) on FACS-purified live

YFP$^+$ and YFP^{neg} keratinocytes from skins of age- and litter-matched control *Krt19CreER; R26-YFP* mice whose postnatal day 50 skins had been treated with tamoxifen during second telogen and then harvested either before wounding (day 0) or at day 80 after wounding (fig. S4A and table S1). After passing quality control metrics (fig. S4B), Leiden clustering of all epithelial cells at day 0 revealed six distinct subsets, readily identified by established markers (*16*, *17*) and underscoring the marked differences between bulge HFSCs and EpdSCs (Fig. 1E and fig. S4, C to E).

Within the UMAP of EpdSC and suprabasal Epd clusters, day-80 bulge-derived wound-experienced *Krt19CreER;R26YFP*$^+$ cells overlaid with day-80 unwounded native EpdSCs (Fig. 1E, lower inset). Among >16,000 detected genes, DESeq2 (*18*) revealed no significant differences in expression (Fig. 1E, right panels). These analyses showed that the transcriptomes of HF-derived and native EpdSCs were virtually indistinguishable; this was further confirmed by pseudospace analysis, where quantification of the relative position of each cell in the UMAP showed no difference (fig. S4F). Thus, despite originating from a markedly distinct niche in which they displayed a very different transcriptome and performed distinct regenerative tasks, bulge HFSCs (uniquely *Krt19YFP*$^+$) responded to injury by re-epithelializing missing epidermis and establishing residence within a new niche. Given the comparable transcriptomes of HF-derived EpdSCs and native EpdSCs, it was not surprising that HF-derived EpdSCs were able to generate and maintain the skin's barrier.

SCs adapt to their new niche after repair

Probing deeper for differences between HF-derived and native EpdSCs, we turned to the chromatin level. We performed ATAC-seq (assay for transposase-accessible chromatin using sequencing) (*19*) on FACS-purified HFSCs isolated during the repair and recovery process (Fig. 2A and fig. S5A). Principal components analyses revealed close clustering among replicates, the expected ATAC peaks centered around transcription start sites (TSSs) and CTCF chromatin looping sites, and peak distribution patterns were comparable across genomic regions (fig. S5, B to D). Genes associated with ATAC peaks were assigned first by proximity using the Genomic Regions Enrichment of Annotations Tool (GREAT) and then refined according to transcript status in bulge HFSCs, wound-activated SCs, and/or EpdSCs (*12*, *13*, *17*).

Before injury, >9000 chromatin peaks distinguished quiescent bulge HFSCs from homeostatic EpdSCs (Fig. 2B). Nearly 6000 peaks were lost within 3 days after wounding. Lost peaks associated with genes such as *Nfix* and *Lhx2*, which are essential for bulge identity and whose expression is known to be rapidly downregulated upon wounding (Fig. 2, B to D, and table S2) (*20*, *21*). We observed that 2360 HFSC peaks were maintained throughout the repair process before waning, including peaks associated with "lineage infidelity" genes such as *Sox9* and the WNT receptor–signaling gene *Tcf7l1* (TCF3) (*22*). Long after repair, however, ~1000 peaks established in bulge HFSCs remained open in HF-derived EpdSC chromatin (Fig. 2B). We address their importance later.

Although many HFSC chromatin peaks closed during and after wound repair, >11,000 chromatin peaks were gained. Associating with EpdSC-expressed genes, >4000 peaks were induced by day 3 after wounding, in agreement with the known induction of epidermal lineage markers by migrating bulge HFSCs during wound repair ("lineage infidelity") (*12*) (Fig. 2, B and E). Even though the wound had closed by day 7, nearly 4000 homeostatic EpdSC-specific chromatin peaks only became accessible after the HF-derived EpdSCs had adapted to their new niche. Notably, these "niche-adaptive" peaks were associated with epidermal differentiation (*Gata3*, *Krt10*), barrier function (*Scd1*, *Lce1l*), and immune defense (*Il20ra*, *Il34*, *Irf4*) genes (Fig. 2C and table S3), reflecting the newly acquired tasks of HF-derived EpdSCs, namely skin barrier maintenance and sentinels to sense barrier breaches and recruit an immune response.

Some niche-adaptive peaks displayed heightened or even unique accessibility in HF-derived EpdSCs over that of native EpdSCs (Fig. 2F and fig. S6A). Because many of these peaks associated with epidermal differentiation and immune defense genes (Fig. 2C and table S4), their openness seemed to reflect "compensatory adaptation," which suggests that HF-derived EpdSCs may remodel these genes to a more open chromatin state in order to transcribe the requisite levels needed to perform their new homeostatic tasks. In this way, HF-derived EpdSCs may be able to compensate for deficiencies in perceiving local environmental cues the way their native counterparts do. This notion was in agreement with the several days' delay relative to native EpdSCs in establishing the barrier after re-epithelialization (Fig. 1C).

Epigenetic wound memories of inflammation and migration

The distinct post-repair configuration of a foreign stem cell's chromatin relative to its native counterparts led us to wonder whether other kinds of epigenetic rearrangements might have occurred within these immigrants. Around 2500 peaks became accessible only after bulge HFSCs experienced the wound, but these peaks were retained in HF-derived EpdSCs after re-epithelialization (Fig. 3A and fig. S6A). Because these peaks were not a feature of native EpdSCs and their associated genes returned to baseline transcription levels after wound closure, they appeared to represent an epigenetic memory of the wound experience.

Wounds are known to induce inflammation, and this was reflected in the enrichment of immune-related genes and pathways for wound memory peaks (Fig. 3A and table S5). Topical skin treatment with imiquimod (IMQ), a psoriasis mimetic drug, induces long-lasting inflammatory-sensitive chromatin peaks within EpdSC chromatin independent of B and T lymphocytes and macrophages (*23*). We therefore looked at the ATAC peaks that were induced in IMQ-exposed EpdSCs and then retained at day 30 after inflammation (fig. S6B) and found them to also be more accessible in HF-derived EpdSCs (Fig. 3B). First described as "trained immunity" in short-lived macrophages, inflammatory memory peaks in EpdSC chromatin sensitize their associated genes to respond more robustly to secondary inflammatory assaults (*24*, *25*).

In contrast, the large number of wound-induced memory ATAC peaks in our study went beyond those described for inflammatory memory. Many of these memory-associated genes encoded cytoskeletal organization and Rho signaling/actomyosin-regulated proteins essential for the extensive polarized cell migration that occurs during re-epithelialization (*26*–*28*) (Fig. 3A and table S5). This aspect of the wound response is not encountered when stem cells are simply exposed to a topical inflammatory stimulus.

To test the physiological relevance of this facet of the wound memory, we first examined the ability of wound-experienced HF-derived epidermis to respond to secondary wound closure in vivo. Relative to naïve native epidermis, wound-experienced HF-derived EpdSCs closed wounds markedly faster (Fig. 3C). As the rates of ethynyl-2′-deoxyuridine (EdU) incorporation were comparable (fig. S6C), the accelerated rate of wound closure appeared to reflect enhanced migration rather than proliferation. Indeed, at the wound front, the polarized epidermal tongue marked by migration-specific integrin α5 was significantly more pronounced in HF-derived epidermal wounds (Fig. 3D). Ex vivo assays further corroborated the enhanced migration of the HF-derived epidermis out of skin explants and revealed more robust signs of membrane ruffling, a hallmark of enhanced Rho/Rac-mediated actomyosin dynamics (fig. S6D) (*29*, *30*).

To test whether the enhanced epithelial migration is intrinsic to HF-derived EpdSCs, we isolated day-80 HF-derived and native EpdSCs by FACS and adapted them to 2D culture conditions wherein no supporting cells were present (fig. S6E). Although no overt differences were observed during propagation (fig. S6F), when scratch-wounded in the presence of mitomycin C to block proliferation, HF-derived EpdSCs were significantly more efficient than their native EpdSC counterparts at migrating in and closing the gap (Fig. 3E and fig. S6G). Moreover, fluorescence microscopy and live imaging of wound-experienced green fluorescent protein (GFP)–actin$^+$ HF-derived EpdSCs

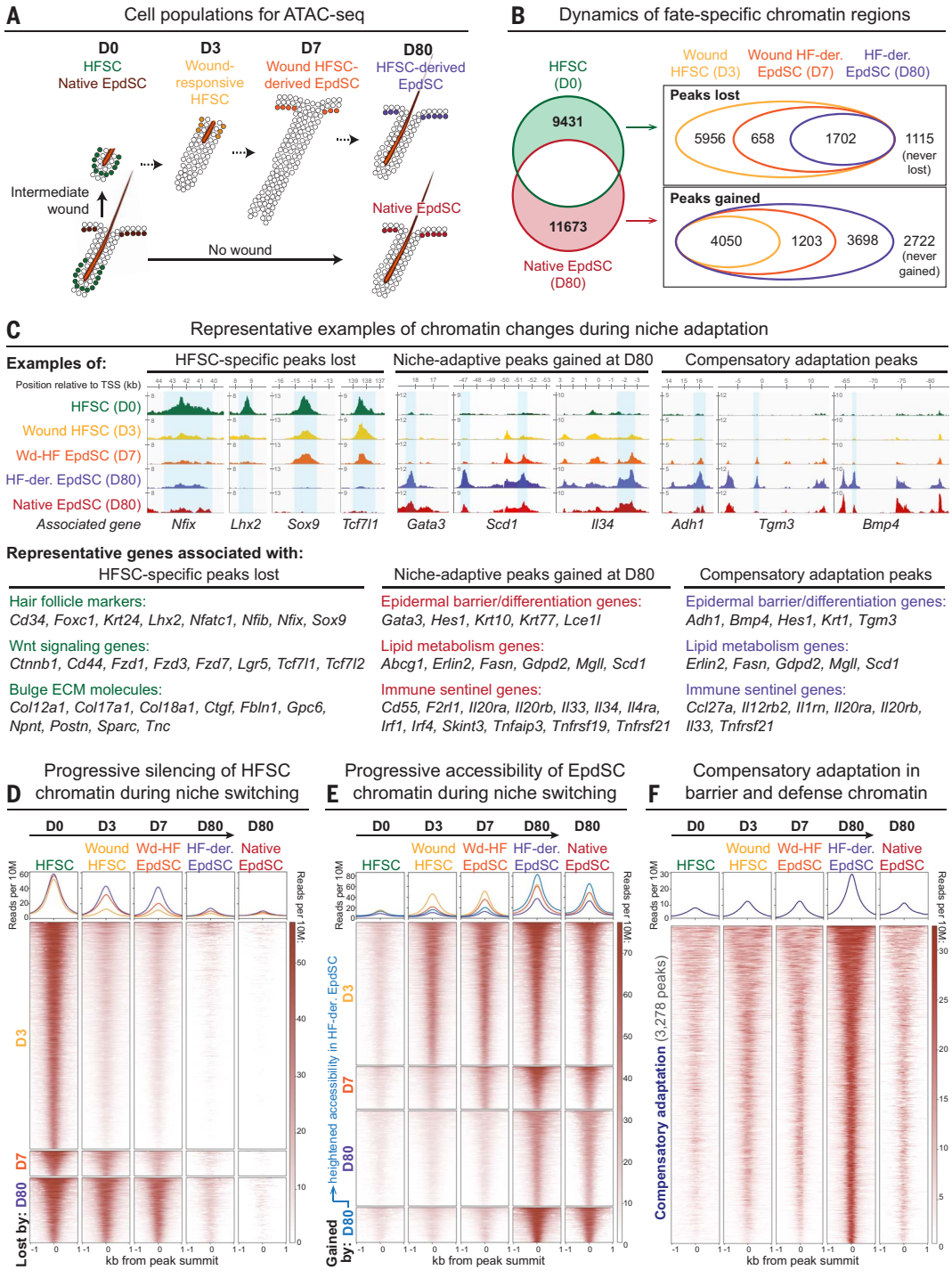

Fig. 2. Stem cell fate switch requires epigenetic adaptation to the new niche. (**A**) Cell populations collected for ATAC-seq analysis (see fig. S4A). (**B**) Venn diagrams depicting the categorization of niche-specific peaks as they are progressively gained or lost over time. Peaks that fluctuate over time were excluded. (**C**) Top: Snapshots of example genomic loci for HFSC-specific peaks lost, EpdSC-specific peaks gained only at day 80 ("niche-adaptive"), and peaks unique to HF-derived EpdSCs ("compensatory adaptation"). Light blue shading denotes called peaks. Bottom: Representative genes for each aforementioned category, grouped by function. (**D** to **F**) Density plots depicting ATAC-seq signals at summits ± 1 kb of HFSC-specific peaks (D), EpdSC-specific peaks (E), and peaks unique to HF-derived EpdSCs (F), with heatmaps of individual peaks beneath.

further corroborated features of active collective cell migration, including membrane ruffling, prominent integrin-mediated focal adhesions, and polarized actin at the leading edge of the migrating front (fig. S6, H and I, and movies S1 and S2) (*26*, *29*, *30*). These findings underscored the cell-intrinsic features of the enhanced performance of wound-experienced HF-derived EpdSCs unleashed upon exposure to a secondary wound environment.

Also noteworthy was the finding that although wound memory genes are largely transcriptionally silent during homeostasis, they became reactivated upon a secondary wound. Moreover, as shown by scRNA-seq analyses, the responsiveness of many memory genes was even more robust within the $\alpha5$-integrin^{+} migrating tongue of secondary wounds (HF-derived EpdSCs) than in primary wounds (native EpdSCs) (Fig. 3F, fig. S7, and table S6). Further underscoring the potential importance of this finding, up-regulated genes were involved in actin cytoskeleton organization, Rho signaling, angiogenesis, tissue growth, and inflammation—all processes important for wound healing (fig. S7F and table S7).

HF-derived EpdSCs remember their niche origin

Curiously, 834 ATAC peaks were characteristic of homeostatic bulge HFSC chromatin and had maintained accessibility throughout both

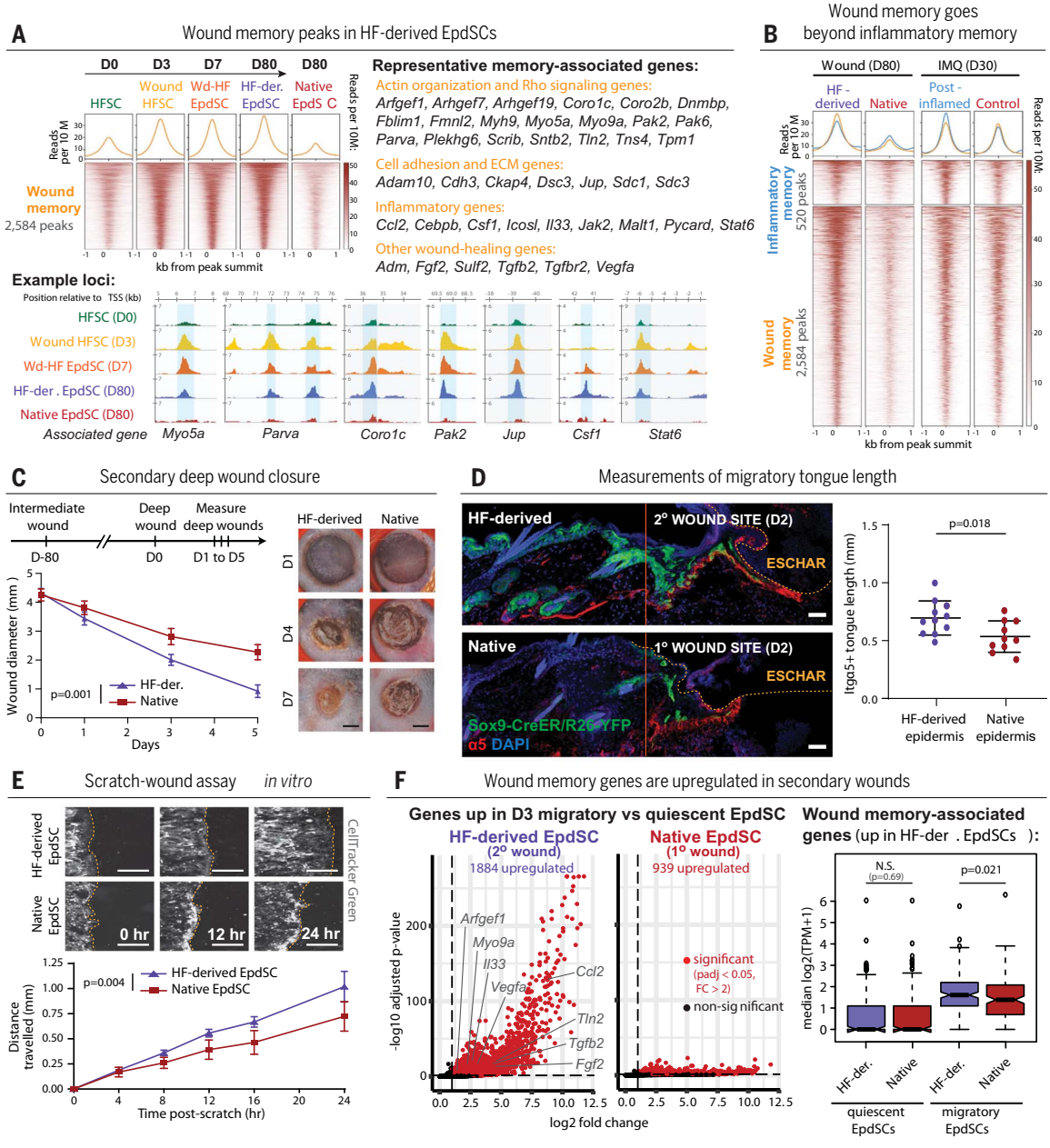

Fig. 3. Wound memory intrinsically accelerates migration kinetics in secondary wounds. (**A**) Density plots depict ATAC-seq signals at summits ± 1 kb of wound memory peaks with heatmap of individual peaks beneath. Representative genes are shown at right. At bottom are snapshots of genomic loci; light blue shading denotes called wound memory peaks. (**B**) Density plots depict ATAC-seq signals at summits ± 1 kb of inflammatory and wound memory peaks, with corresponding heatmaps of individual peaks below. Inflammatory memory peaks were called by reanalyzing data from post-inflamed IMQ-treated skin in (*23*) (see fig. S6B and supplementary materials). Note that the 520 inflammatory memory peaks exhibit similar memory in HF-derived EpdSCs at day 80 after wounding, but the 2584 memory peaks induced by wounding were relatively unchanged between post-inflamed EpdSCs and their untreated control. (**C**) Secondary deep wound closure assays. Timeline of the experiment is shown at top left, quantification of wound closure rates at bottom left, and representative photographs of wounds at right. Scale bars, 2 mm. Error bars denote SD from 11 (HF-derived) or 10 (native) wounds. Simple linear regression was used to calculate *P* value between slopes. (**D**) Representative immunofluorescence images of wound edge 2 days after a secondary deep wound administered to either HF-derived re-epithelialized day-80 epidermis or native epidermis. Vertical lines denote boundaries of the wound. Orange dashed line denotes the epidermis-eschar boundary. Scale bars, 50 μm. Quantification of migrating $\alpha5^+$ tongue length is at right. Error bars denote SD from 11 (HF-derived) or 10 (native) wound edges. Unpaired *t* test was used to calculate *P* value. (**E**) Top: Representative images of proliferation-blocked (by mitomycin C) cell migration into a large scratch wound (~2.5 mm), as tracked by CellTracker Green at the times indicated. Dashed lines denote migratory border. Scale bars, 0.5 mm. Bottom: Quantification of distance traveled over time. Error bars denote SD from 10 (HF-derived) or 14 (native) scratch wounds. Simple linear regression was used to calculate *P* value between slopes. (**F**) Left: DESeq2 analysis of EpdSCs collected 3 days after deep wounding. Shown are genes whose expression is up-regulated in migratory versus quiescent clusters (see fig. S7, D and E). Representative genes with wound memory peaks are marked, highlighting their more robust transcription in the secondary versus primary wound. Right: Boxplot of median transcript levels as $\log_2$ (TPM+1) values of 202 wound memory–associated genes whose expression is up-regulated specifically in the migratory tongue of HF-derived EpdSCs in secondary wounds. Boxplot central line denotes the median, boxes denote the interquartile range (IQR), and whiskers denote 1.5 × IQR. Mann-Whitney test was used to calculate *P* value.

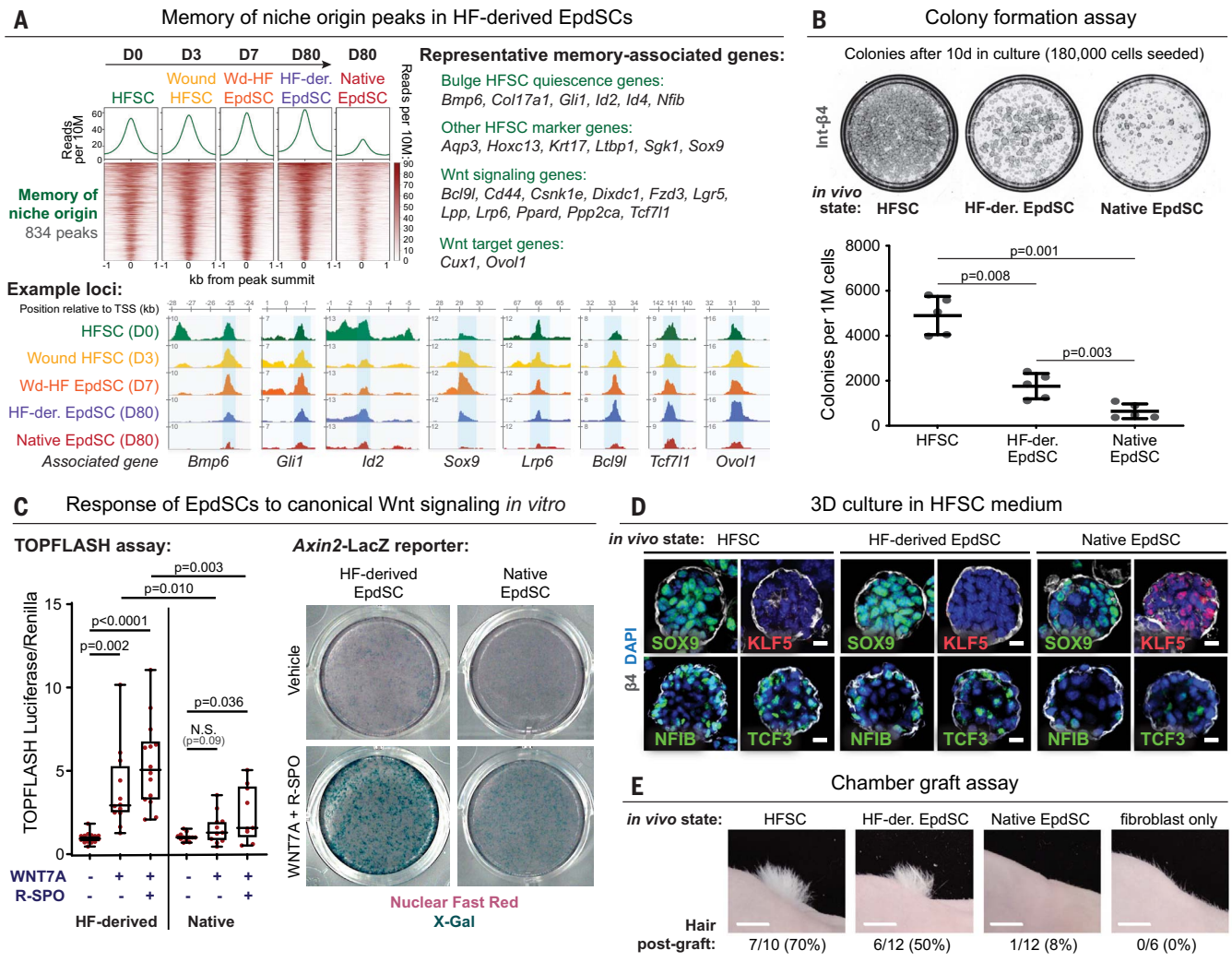

Fig. 4. Memory of niche origin enables efficient reversion to HFSCs. (**A**) Density plots depict ATAC-seq signals at summits ± 1 kb of memory-of-niche-origin peaks with heatmap of individual peaks beneath. Representative genes are shown at right; at bottom are snapshots of genomic loci; light blue shading denotes called HFSC memory peaks. (**B**) Colony-forming assays. Colonies (immunolabeled for integrin-β4) formed at 10 days after seeding freshly FACS-isolated SCs from skins onto culture conditions that mimic an activated HFSC state. Quantifications are shown beneath images. Error bars denote SD from five cell derivations. Paired *t* test was used to calculate *P* value. (**C**) Canonical WNT response to 24 hours of treatment with WNT7a and R-spondin1 in cultures of HF-derived and native EpdSCs. Left: TOPFLASH luciferase assay. Boxplot whiskers denote min-max, boxes denote 25th to 75th percentiles, and central line denotes the median. Numbers of replicates from left to right: 17, 12, 14, 13, 11, 9. Welch's *t* test was used to calculate *P* value. Right: Scans of X-gal staining of Axin2-LacZ reporter cell lines (in 24-well plates). (**D**) Representative images of SCs cultured as 3D spheroids that mimic a quiescent bulge-like state. Green immunolabeling is for SOX9, NFIB and TCF3, whose genes have memory-of-bulge origin peaks. Red indicates KLF5, an EpdSC marker. Scale bars, 20 μm. (**E**) Representative photographs of de novo hairs that developed 2 months after grafting (chamber grafts) of SCs cultured under activated HFSC conditions. Scale bars, 0.5 cm. Numbers of grafts displaying substantial hair growth are shown at bottom.

wound repair and epidermal adaptation of HF-derived EpdSCs (Fig. 4A). On the basis of this behavior and their relative paucity in native EpdSCs, these peaks in HF-derived EpdSC chromatin appeared to reflect an epigenetic memory of their bulge niche origin.

The top Gene Ontology term categories in this cohort were known to be important in HFSC and hair formation (table S8). These memory domains were associated with key genes regulating bulge HFSC quiescence, such as *Bmp6*, *Sox9*, *Nfib*, *Col17a1*, *Id2*, and *Gli1*, and also bulge-enriched genes essential for WNT signaling–mediated activation of HFSCs to launch the hair cycle, such as *Tcf7l1*, *Lgr5*, *Lpp*, *Fzd1*, and *Lrp6* (*22*, *31*–*33*) (Fig. 4A). Although these genes were not transcribed by HF-derived EpdSCs during normal skin homeostasis, we wondered whether this epigenetic memory might endow the cells with a heightened propensity to unleash an HFSC-like behavior when challenged to do so.

Through mechanisms poorly understood, HFSCs are known to possess higher WNT sensitivity than EpdSCs and display greater colony-forming efficiency and passaging potential when placed in culture under conditions that favor a lineage-activated ("hair germ") state (*4*). True to their HF origins but distinct from native EpdSCs, HF-derived EpdSCs were more efficient in forming colonies (Fig. 4B). Additionally, in response to R-spondin1 and WNT7a, an established canonical WNT in regeneration and wound repair (*33*), HF-derived EpdSCs showed an increased sensitivity to WNT signaling, characteristic of activated HFSCs (Fig. 4C and fig. S8, A to C).

In their quiescent state, bulge HFSCs are in a WNT-restricted niche, where they express

transcription factors (TFs) such as SOX9 and NFIB/X, which function in maintaining HFSCs and preventing EpdSC conversion (*20*). Bulge HFSCs also express TCF3, which is essential to mediate WNT-responsive HFSC activation to launch hair cycling (*22*). These genes were associated with memory of bulge niche origin, and when we switched to culture conditions that mimic quiescent bulge HFSCs in their native niche, HF-derived EpdSCs up-regulated the nuclear expression of SOX9, TCF3, and NFIB and down-regulated that of EpdSC TF KLF5 (Fig. 4D and fig. S8D). Thus, HF-derived EpdSCs retained their potential to respond to WNTs and bulge niche–promoting conditions even after taking up residence long term in the epidermal niche. Because the transcriptomes of HF-derived EpdSCs and EpdSCs within the homeostatic epidermal niche in vivo were indistinguishable, the thread connecting HFSCs and HF-derived EpdSCs appeared to be the >800 "memory of origin domains" associated with genes such as *Tcf7l1*, *Nfib*, and *Sox9* that became reactivated upon secondary exposure to a bulge microenvironment.

We reasoned that if the collective "memory of bulge niche origin" is functionally important in skin physiology, it should confer an increased ability of HF-derived EpdSCs to regenerate hair in vivo. We tested this possibility with "chamber graft" assays in which we combined our cultured stem cell populations with neonatal dermal fibroblasts and engrafted them onto hairless (*Nude*) mice (*4*). In contrast to GFP-marked EpdSCs, which generated primarily epidermis in grafts, GFP-marked HF-derived EpdSCs formed both epidermis and hair efficiently (Fig. 4E and fig. S8E). These de novo hairs were replete with WNT-activated HF morphogenesis preceding hair production (fig. S8, E and F). Together, these data provide compelling evidence that HF-derived EpdSCs maintain a memory of their niche origin, and after engraftment in vivo, this memory endows them with a broadened tissue-regenerating capacity.

Insights into the multiplicity of memories, their diversity, and their ability to accumulate

We next turned to addressing how memory domains are established in space and time, and what maintains them in a poised open state when their environment shifts. We first analyzed the TF sequence motifs encompassed within ATAC peaks that are open exclusively in one particular state and then resolved in subsequent environments (Fig. 5A, fig. S9A, and table S9). As expected, the ATAC peaks exclusive to quiescent bulge HFSCs were enriched for motifs that bind bulge identity TFs (LHX2, NFIB/X, NFATc1, SOX9), wound-specific peaks were enriched for the binding of wound TFs (AP-1, CEBP, ATF/CRE, NFκB/REL), and EpdSC-specific peaks were enriched for the binding of EpdSC TFs (KLF5, GATA3, GRHL) (Fig. 5A). With the exception of the dual expression of EpdSC and HFSC TF genes during the lineage infidelity period of the wound response (*12*), the expression patterns of TFs correlated with this state specificity (Fig. 5B).

Displaying the greatest complexity in TF motifs were the memory-of-bulge-origin peaks; they showed enrichment for the binding of TFs from all three states (Fig. 5, A and B, and table S9). In this regard, they differed from lineage-infidelity ATAC peaks, which were typified by sequence motifs for HFSC-specific and wound-specific TFs but lacked those for EpdSC-specific TF motifs (fig. S9B and table S9). Although memory-of-bulge-origin ATAC peaks were already open in bulge HFSCs and remained open throughout environmental shifts, wound memory peaks opened de novo upon wounding. These domains were highly enriched for STAT and C/EBP, which have been implicated as key pioneer factors in opening inflammatory memory chromatin (*34*, *35*). Like all of the memory domains analyzed, wound memory peaks were also typified by the presence of motifs for the chromatin remodeling factor AP-1 (*36*, *37*) and EpdSC TF KLF5.

Finally, niche-adaptive and compensatory adaptation peaks were typified by the same binding motifs as native EpdSC peaks (Fig. 5A, fig. S9B, and table S9). Although knowledge of chromatin dynamics in the epidermis is still scant, this provides an explanation for how these peaks open only after re-epithelialization. These peaks show an enrichment for AP-1, which is also induced in a variety of stress situations. It will be interesting to probe whether adaptation entails a transient stress period during which these sites open and HF-derived EpdSCs adjust to their new environment.

Another intriguing feature of memory domains is that they tended to be within intergenic regions, likely enhancers, that are more open than their state-specific counterparts at the time when their establishment took place (fig. S9, C and D). We posit that this might extend the accessibility of these domains as stem cells transition from one environment to another, thereby facilitating the binding of new state-specific TFs as the expression of others wanes and maintaining the open chromatin state across these dynamics.

Our transcriptomic analysis of primary versus secondary wounds (Fig. 3F) suggests that the memory and niche adaptation domains identified here act similarly to inflammatory memory domains in that their associated genes are generally dormant unless these memory enhancers are triggered by reexposure to the stimulus that prompted their activation (*25*). To further bolster this point and establish a more direct connection between memory peaks and their environment-sensing activity, we selected some of the most accessible memory/adaptation domains and used them as enhancers to drive eGFP in mice (fig. S9E). These domains functioned faithfully in driving reporter expression in a state-specific manner that corresponded both to the cell's environmental experience within the skin and to the natural transcriptional status of the genes associated with these chromatin peaks (Fig. 5C and fig. S9, F to H). Although we could not appraise the heightened accessibility of compensatory adaptation peaks by this assay, we did find that peaks associated with compensatory adaptation were active in only epidermis and not HF or wound states. Overall, these results underscore the physiological relevance of memory/adaptation domains in gene governance.

Finally, if these epigenetic memories are truly dependent on a stem cell's prior experiences, then memories of wound and bulge niche origin should be uncoupled in re-epithelialized epidermis derived from wound-mobilized EpdSCs (deep wound) as compared to wound-mobilized bulge HFSCs (intermediate wound). Indeed, by ATAC-seq analyses, whereas wound memory domains were comparable, epidermis from wound-mobilized EpdSCs lacked robust HFSC memory domains (Fig. 5D and fig. S10, A to E). Chromatin changes associated with compensatory adaptation to the epidermal niche were also markedly different in HF-derived EpdSCs versus epidermal-derived EpdSCs (fig. S10F).

Consistent with their wound memory, wound-experienced epidermal-derived EpdSCs exhibited enhanced performance over their unwounded counterparts at wound closure both in vivo and in vitro (Fig. 5E and fig. S10, G and H). However, and in contrast to wound-experienced HF-derived EpdSCs, the sensitivity of wound-experienced epidermal-derived EpdSCs to WNTs and to hair regeneration in engraftments was no better than their native EpdSC counterparts (Fig. 5F and fig. S10I). These data provide functional evidence in support of the experience-dependent and cumulative nature of epigenetic memories and their physiological relevance in conferring heightened secondary responses to subsequent exposure to the environmental conditions that stimulated their establishment.

Discussion

Because long-lived adult stem cells can harbor inflammatory memory (*23*, *25*, *34*), we examined whether they might also possess memories of different kinds of experiences, and if so, whether such memories are cumulative. Wounding under conditions where bulge HFSCs were the primary responders to long-term epidermal repair offered an opportunity to monitor these tissue stem cells as they encountered a series of diverse experiences, first exiting their HF niche, then encountering inflammation as they migrated into the wound bed, then re-epithelializing the vacated epidermis, and

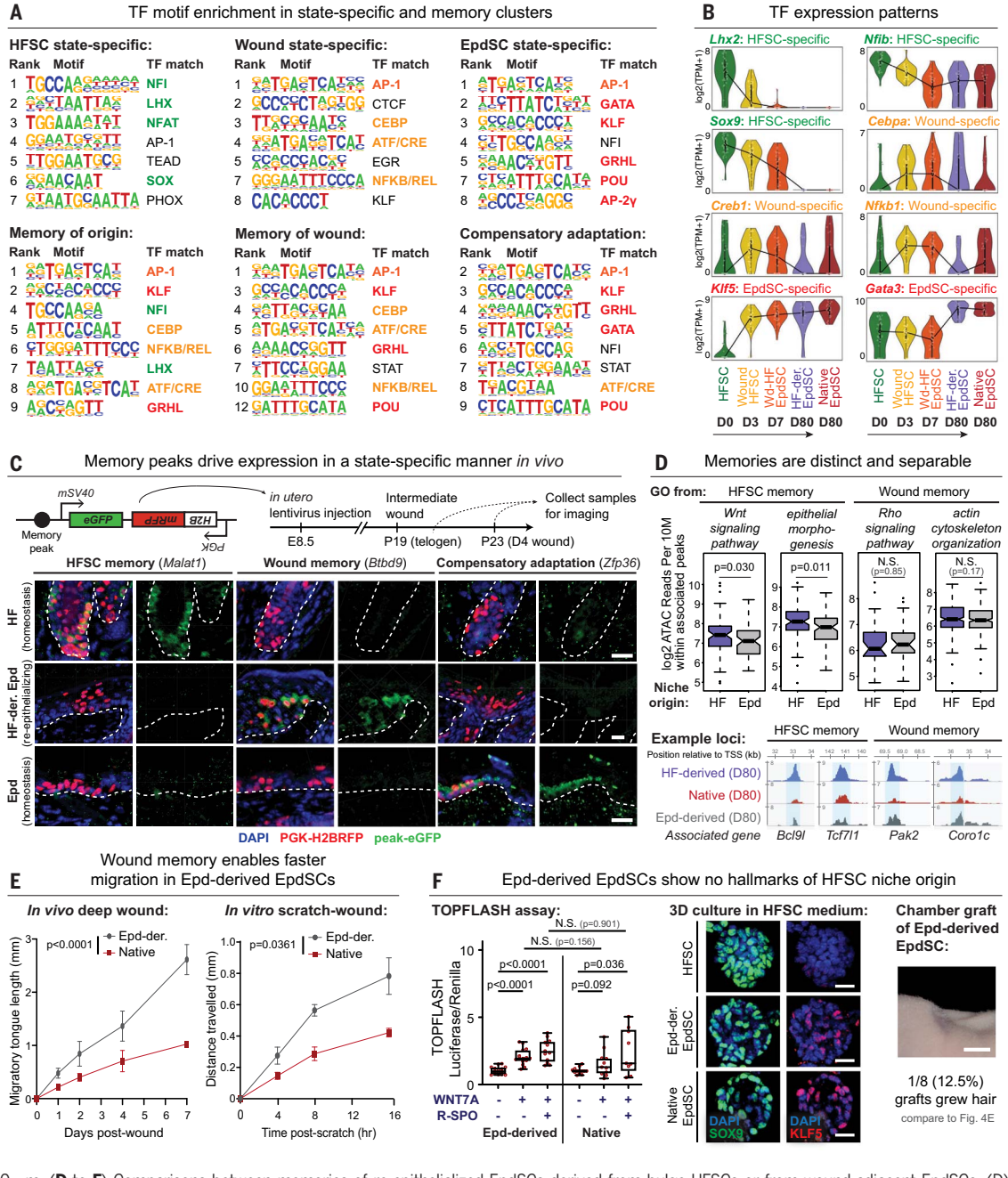

Fig. 5. Epigenetic memories are distinct, separate, and cumulative. (**A**) Transcription factor motifs that are enriched in state-specific ATAC peaks (see fig. S9A) and memory peaks, based on de novo motif discovery by HOMER against genomic background. Significant motifs with a match score of >0.8 to a known motif are ranked (see table S9). (**B**) Differential TF expression in vivo. Data are shown as violin plots of transcript levels as $\log_2$ (TPM+1) values of representative TFs with motifs from (A). (**C**) Functional tests of memory peaks. Top: Experimental strategy. Lentiviruses harboring memory peak–driven GFP reporters and *Pgk*-H2BRFP (to track transduced cells) were delivered in utero, and skin samples of adult transduced mice were analyzed before and after intermediate wounding. Bottom: Representative images show state-specific reporter activities. Note that for the compensatory adaptation reporter, the cloned locus is associated with a gene expressed in native EpdSCs, but here is integrated randomly in the genome; positive expression of the reporter is reflective of the absence of other peaks in its vicinity that normally drive the gene's expression in the unwounded state. Scale bars, 20 μm. (**D** to **F**) Comparisons between memories of re-epithelialized EpdSCs derived from bulge HFSCs or from wound-adjacent EpdSCs. (D) Top: Boxplot of chromatin accessibility in peaks associated with memory in HF-derived (intermediate wound) and Epd-derived (deep wound) EpdSCs. Values are plotted from the union of peaks in each equivalent memory type (see fig. S10E), subdivided according to their association with genes in each relevant Gene Ontology term. Boxplot central line denotes the median, boxes denote IQR, and whiskers denote 1.5 × IQR. Mann-Whitney test was used to calculate *P*. Bottom: Snapshots of genomic loci; light blue shading denotes called memory peaks. (E) Memory of wound is independent of niche origin. Quantifications of migration rates after secondary wounds in vivo (left) or scratch wounds in vitro (right) are shown. Error bars denote SD from three in vivo wounds and four in vitro wounds. Simple linear regression was used to calculate *P* value between slopes. (F) Memory of WNT responsiveness and hair regeneration depends on niche origin. Left: TOPFLASH luciferase assay. Boxplot whiskers denote min-max, boxes denote 25th to 75th percentiles, and central line denotes the median. Numbers of replicates from left to right: 15, 15, 12, 13, 11, 9. Welch's *t* test was used to calculate *P*. Center: Representative images of 3D spheroids immunolabeled for SOX9 and KLF5. Scale bars, 20 μm. Right: Representative photograph of chamber graft 2 months after grafting of cultured Epd-derived EpdSCs. Scale bar, 0.5 cm. Compare numbers of grafts displaying substantial hair growth to Fig. 4E.

eventually taking up long-term residence there. A remarkable facet of this choreographed process is that these SCs gained epigenetic memories of their diverse experiences at each step along the way.

These memories were both distinct and cumulative. For each environmental encounter, certain chromatin domains within key temporally regulated gene enhancers became highly accessible and then remained accessible long after the experience and after normal physiology had been restored. Moreover, each memory that had been acquired and stored along the way endowed the stem cell with distinct physiological advantages that were dormant

during normal homeostasis, but then become unleashed upon a secondary challenge. Thus, HF-derived EpdSCs now residing as permanent immigrants in the epidermis behaved like their native EpdSC counterparts, right down to their equivalent transcriptomes. However, when roused to self-renew, regenerate skin tissues, or provide a secondary wound response, wound-experienced HF-derived EpdSCs outperformed normal EpdSCs. These features are classical ones of trained immunity, where some epigenetic marks of an inflammatory response are retained after exposure, priming the cell to respond more quickly to a subsequent exposure (*24*, *25*).

The epigenetic memories revealed here are separable, varying according to a stem cell's past experiences. Thus, when EpdSCs were mobilized to repair deep wounds, they retained a wound memory similar to HFSCs that were mobilized to repair intermediate wounds. However, only HF-derived EpdSCs possessed a memory of their HF origin. Moreover, although EpdSCs underwent some chromatin remodeling after their re-epithelialization of a deep wound, this adaptation differed markedly from the compensatory adaptation exhibited by HF-derived EpdSCs. These findings further support the notion that sustaining a transcriptome akin to native EpdSCs and performing the task of fueling the skin's barrier remained an adaptation challenge for these former HF residents in a way not experienced by wound-mobilized EpdSCs.

Finally, we showed that these epigenetic memory domains possess characteristics that are adjusted to suit their particular past experiences. In cases such as *Sox9*, whose TF is required for maintaining HFSC fate as well as lineage infidelity, some ATAC peaks activated in wound-mobilized bulge SCs closed within 3 days, others closed only after re-epithelialization, whereas still others remained open at day 80 after epidermis repair. *Sox9*'s transcriptional profile—more robust in the bulge than in the wound—reflected these features. However, as is common for all genes associated with day 80 memory-of-origin domains, *Sox9* was not expressed in HF-derived EpdSCs until spurred to do so by the right environmental stimuli. In this regard, it was notable that "memory of bulge niche origin" domains possessed motifs for the binding of HFSC, wound, and EpdSC TFs. This enabled the chromatin to adapt to different lineage fates, even after the TFs that initially drove their transcription were silenced.

Repairing injuries is a crucial role for all tissue stem cells. As such, our discovery that stem cells acquire and store functional epigenetic memories of the complex steps involved in wound repair is likely to have implications for tissue fitness and regenerative medicine that go beyond the skin. Our findings imply that epigenetic memories can be maladaptive (as inflammatory memory is likely to be for chronic inflammatory conditions) or beneficial (as the memories of origin, wound repair, and even niche compensatory adaptations that we describe here would appear to be). Although these memories are unlikely to persist forever, it is noteworthy that 2 months in a mouse's life is the equivalent of 5 to 6 years in humans. Thus, the combination of epigenetic adaptations and cumulative acquisition of memories stockpiled within the chromatin of wound-experienced adult stem cells provides an altered view of tissue performance. That said, as desirable as it may be to be able to self-renew longer, repair wounds faster, and broaden the fates of tissue stem cells, these features are also ones associated with malignancies, and as such, they may blur the line between good and bad memories.

Methods summary

Deep, intermediate, and shallow wounding

Adult mice at telogen were anesthetized with isoflurane and treated with buprenorphine prior to wounding. For shallow and intermediate wounds, back skins were first shaved, then treated with hair removal cream (Veet). A Dremel Inc. tool with a polishing wheel was used to generate abrasions by polishing the skin laterally three or four times for shallow wounds and six to eight times for intermediate wounds (Dremel 100-series rotary tool and 520 polishing wheel). For deep wounds, back skins were shaved and wounds were created with a 6-mm punch biopsy tool.

ATAC-seq library preparation and sequencing

ATAC-seq libraries were made from freshly FACS-sorted cells, with two to four biologically independent replicates per cell population. Library preparation was performed as described (*12*). The samples were sequenced on Illumina Nextseq 500 using a 75-bp paired-end-reads setting.

Detailed materials and methods are available in the supplementary materials.

REFERENCES AND NOTES

1. K. A. U. Gonzales, E. Fuchs, Skin and Its Regenerative Powers: An Alliance between Stem Cells and Their Niche. *Dev. Cell* **43**, 387–401 (2017). doi: 10.1016/j.devcel.2017.10.001; pmid: 29161590
2. C. B. Johnson, J. Zhang, D. Lucas, The Role of the Bone Marrow Microenvironment in the Response to Infection. *Front. Immunol.* **11**, 585402 (2020). doi: 10.3389/fimmu.2020.585402; pmid: 33324404
3. S. J. Morrison, A. C. Spradling, Stem cells and niches: Mechanisms that promote stem cell maintenance throughout life. *Cell* **132**, 598–611 (2008). doi: 10.1016/j.cell.2008.01.038; pmid: 18295578
4. C. Blanpain, W. E. Lowry, A. Geoghegan, L. Polak, E. Fuchs, Self-renewal, multipotency, and the existence of two cell populations within an epithelial stem cell niche. *Cell* **118**, 635–648 (2004). doi: 10.1016/j.cell.2004.08.012; pmid: 15339667
5. C. P. Lu *et al.*, Identification of stem cell populations in sweat glands and ducts reveals roles in homeostasis and wound repair. *Cell* **150**, 136–150 (2012). doi: 10.1016/j.cell.2012.04.045; pmid: 22770217
6. G. J. Spangrude, S. Heimfeld, I. L. Weissman, Purification and characterization of mouse hematopoietic stem cells. *Science* **241**, 58–62 (1988). doi: 10.1126/science.2898810; pmid: 2898810
7. J. Stingl *et al.*, Purification and unique properties of mammary epithelial stem cells. *Nature* **439**, 993–997 (2006). doi: 10.1038/nature04496; pmid: 16395311
8. M. Shackleton *et al.*, Generation of a functional mammary gland from a single stem cell. *Nature* **439**, 84–88 (2006). doi: 10.1038/nature04372; pmid: 16397499
9. M. E. Page, P. Lombard, F. Ng, B. Göttgens, K. B. Jensen, The epidermis comprises autonomous compartments maintained by distinct stem cell populations. *Cell Stem Cell* **13**, 471–482 (2013). doi: 10.1016/j.stem.2013.07.010; pmid: 23954751
10. Y. Ge, E. Fuchs, Stretching the limits: From homeostasis to stem cell plasticity in wound healing and cancer. *Nat. Rev. Genet.* **19**, 311–325 (2018). doi: 10.1038/nrg.2018.9; pmid: 29479084
11. M. Ito *et al.*, Stem cells in the hair follicle bulge contribute to wound repair but not to homeostasis of the epidermis. *Nat. Med.* **11**, 1351–1354 (2005). doi: 10.1038/nm1328; pmid: 16288281
12. Y. Ge *et al.*, Stem Cell Lineage Infidelity Drives Wound Repair and Cancer. *Cell* **169**, 636–650.e14 (2017). doi: 10.1016/j.cell.2017.03.042; pmid: 28434617
13. H. Yang, R. C. Adam, Y. Ge, Z. L. Hua, E. Fuchs, Epithelial-Mesenchymal Micro-niches Govern Stem Cell Lineage Choices. *Cell* **169**, 483–496.e13 (2017). doi: 10.1016/j.cell.2017.03.038; pmid: 28413068
14. S. Park *et al.*, Tissue-scale coordination of cellular behaviour promotes epidermal wound repair in live mice. *Nat. Cell Biol.* **19**, 155–163 (2017). doi: 10.1038/ncb3472; pmid: 28248302
15. M. Aragona *et al.*, Defining stem cell dynamics and migration during wound healing in mouse skin epidermis. *Nat. Commun.* **8**, 14684 (2017). doi: 10.1038/ncomms14684; pmid: 28248284
16. S. Joost *et al.*, Single-Cell Transcriptomics Reveals that Differentiation and Spatial Signatures Shape Epidermal and Hair Follicle Heterogeneity. *Cell Syst.* **3**, 221–237.e9 (2016). doi: 10.1016/j.cels.2016.08.010; pmid: 27641957
17. D. Haensel *et al.*, Defining Epidermal Basal Cell States during Skin Homeostasis and Wound Healing Using Single-Cell Transcriptomics. *Cell Rep.* **30**, 3932–3947.e6 (2020). doi: 10.1016/j.celrep.2020.02.091; pmid: 32187560
18. M. I. Love, W. Huber, S. Anders, Moderated estimation of fold change and dispersion for RNA-seq data with DESeq2. *Genome Biol.* **15**, 550 (2014). doi: 10.1186/s13059-014-0550-8; pmid: 25516281
19. J. D. Buenrostro, P. G. Giresi, L. C. Zaba, H. Y. Chang, W. J. Greenleaf, Transposition of native chromatin for fast and sensitive epigenomic profiling of open chromatin, DNA-binding proteins and nucleosome position. *Nat. Methods* **10**, 1213–1218 (2013). doi: 10.1038/nmeth.2688; pmid: 24097267
20. R. C. Adam *et al.*, NFI transcription factors provide chromatin access to maintain stem cell identity while preventing unintended lineage fate choices. *Nat. Cell Biol.* **22**, 640–650 (2020). doi: 10.1038/s41556-020-0513-0; pmid: 32393888
21. R. C. Adam *et al.*, Pioneer factors govern super-enhancer dynamics in stem cell plasticity and lineage choice. *Nature* **521**, 366–370 (2015). doi: 10.1038/nature14289; pmid: 25799994
22. R. C. Adam *et al.*, Temporal Layering of Signaling Effectors Drives Chromatin Remodeling during Hair Follicle Stem Cell Lineage Progression. *Cell Stem Cell* **22**, 398–413.e7 (2018). doi: 10.1016/j.stem.2017.12.004; pmid: 29337183
23. S. Naik *et al.*, Inflammatory memory sensitizes skin epithelial stem cells to tissue damage. *Nature* **550**, 475–480 (2017). doi: 10.1038/nature24271; pmid: 29045388
24. M. Divangahi *et al.*, Trained immunity, tolerance, priming and differentiation: Distinct immunological processes. *Nat. Immunol.* **22**, 2–6 (2021). doi: 10.1038/s41590-020-00845-6; pmid: 33293712
25. R. E. Niec, A. Y. Rudensky, E. Fuchs, Inflammatory adaptation in barrier tissues. *Cell* **184**, 3361–3375 (2021). doi: 10.1016/j.cell.2021.05.036; pmid: 34171319
26. M. Schober *et al.*, Focal adhesion kinase modulates tension signaling to control actin and focal adhesion dynamics. *J. Cell Biol.* **176**, 667–680 (2007). doi: 10.1083/jcb.200608010; pmid: 17325207
27. M. D. Kubler, F. M. Watt, Changes in the distribution of actin-associated proteins during epidermal wound healing. *J. Invest. Dermatol.* **100**, 785–789 (1993). doi: 10.1111/1523-1747.ep12476492; pmid: 8388426
28. X. L. Strudwick, A. J. Cowin, Multifunctional Roles of the Actin-Binding Protein Flightless I in Inflammation, Cancer and

Wound Healing. *Front. Cell Dev. Biol.* **8**, 603508 (2020). doi: 10.3389/fcell.2020.603508; pmid: 33330501
29. S. Raghavan, A. Vaezi, E. Fuchs, A role for alphabeta1 integrins in focal adhesion function and polarized cytoskeletal dynamics. *Dev. Cell* **5**, 415–427 (2003). doi: 10.1016/S1534-5807(03)00261-2; pmid: 12967561
30. S. Etienne-Manneville, A. Hall, Rho GTPases in cell biology. *Nature* **420**, 629–635 (2002). doi: 10.1038/nature01148; pmid: 12478284
31. Y. S. Choi *et al*., Distinct functions for Wnt/β-catenin in hair follicle stem cell proliferation and survival and interfollicular epidermal homeostasis. *Cell Stem Cell* **13**, 720–733 (2013). doi: 10.1016/j.stem.2013.10.003; pmid: 24315444
32. V. Greco *et al*., A two-step mechanism for stem cell activation during hair regeneration. *Cell Stem Cell* **4**, 155–169 (2009). doi: 10.1016/j.stem.2008.12.009; pmid: 19200804
33. M. Ito *et al*., Wnt-dependent de novo hair follicle regeneration in adult mouse skin after wounding. *Nature* **447**, 316–320 (2007). doi: 10.1038/nature05766; pmid: 17507982
34. B. de Laval *et al*., C/EBPβ-Dependent Epigenetic Memory Induces Trained Immunity in Hematopoietic Stem Cells. *Cell Stem Cell* **26**, 793 (2020). doi: 10.1016/j.stem.2020.03.014; pmid: 32386557
35. C. M. Lau *et al*., Epigenetic control of innate and adaptive immune memory. *Nat. Immunol.* **19**, 963–972 (2018). doi: 10.1038/s41590-018-0176-1; pmid: 30082830
36. T. Vierbuchen *et al*., AP-1 Transcription Factors and the BAF Complex Mediate Signal-Dependent Enhancer Selection. *Mol. Cell* **68**, 1067–1082.e12 (2017). doi: 10.1016/j.molcel.2017.11.026; pmid: 29272704
37. S. B. Larsen *et al*., Establishment, maintenance, and recall of inflammatory memory. *Cell Stem Cell* **28**, 1758–1774.e8 (2021). doi: 10.1016/j.stem.2021.07.001; pmid: 34320411

ACKNOWLEDGMENTS

We thank J. Levorse and J. Racelis for technical support and C. Lu, M. Laurin, S. Ellis, K. Stewart, H. Yang, N. Gomez, Y. Yang, A. Bonny, and S. Gur-Cohen for discussions. FACS was conducted by Rockefeller University's Flow Cytometry Core (S. Svetlana, director); ATAC-seq and RNA-seq were conducted by RU's Genomics Core (C. Zhao, director); all mouse work was performed in RU's Center for Comparative Biology and under ALAAC accreditation and according to guidelines for animal care set by NIH. **Funding:** Supported by Cancer Research Institute Carson Family Fellowship, Bristol-Myers Squibb Fellowship, and Human Frontier Science Program Long-Term Fellowship (K.A.U.G.); NIH Ruth Kirstein Postdoctoral Fellowship (1F32AR073105) and Glenn Foundation for Medical Research Postdoctoral Fellowship in Aging Research (M.T.T.); Damon Runyon Cancer Research Foundation National Mah Jongg League Fellowship DRG 2409-20 (A.G.); National Institute of Arthritis and Musculoskeletal and Skin Diseases National Research Service Award F31AR073110 (N.R.I.); Damon Runyon Cancer Research Foundation Fellowship, Rockefeller Women & Science Postdoctoral Fellowship, Jane Coffin Childs Memorial Fund, and NIH K99 Transitional Award (AR072780-02) (S.Liu); Weill Cornell/Rockefeller/Sloan Kettering Tri-Institutional Medical Scientist Training Program Predoctoral Fellowship T32GM007739 and NIH F30 fellowship 1 F30 HD107964-01 (J.S.S.N.); Agency for Science, Technology and Research (A*STAR) Singapore Fellowship (K.L.); and National Institute of Arthritis and Musculoskeletal and Skin Diseases awards R01-AR050542, R01-AR31737, and R01-AR27833 (E.F.). E.F. is an investigator of the Howard Hughes Medical Institute.

Author contributions: Conceptualization and writing original draft, K.A.U.G. and E.F.; methodology, K.A.U.G., L.P., I.M., M.T.T., A.G., E.F.; investigation of wounding in mice, L.P.; live and confocal imaging, I.M.; 3D culture and reporter testing in vitro, M.T.T.; whole-mount imaging, A.G.; reporter cloning and lentivirus packaging, E.W.; scRNA-seq for secondary wounds, ATAC-seq library prep for deep wounds, N.R.I.; dermal fibroblast isolation for chamber grafts, M.N.; flow cytometry for stem cell compartment contributions, S.Luo, S.Lu., and K.L.; experiments for revision, J.S.S.N.; toluidine blue staining, H.A.P.; all other experiments, including software and formal analysis, K.A.U.G.; funding acquisition and supervision, E.F. All authors read and edited the final manuscript. **Competing interests:** The authors declare that they have no competing interests. **Data and materials availability:** RNA- and ATAC-sequencing data from this study have been deposited in the Gene Expression Omnibus (www.ncbi.nlm.nih.gov/geo/) under accession codes GSE165312 and GSE165314. All other data in the manuscript, supplementary materials, and source data are available from the corresponding author upon reasonable request.

SUPPLEMENTARY MATERIALS

science.org/doi/10.1126/science.abh2444
Materials and Methods
Figs. S1 to S10
Tables S1 to S9
References (*38*–*61*)
Movies S1 and S2
MDAR Reproducibility Checklist

View/request a protocol for this paper from *Bio-protocol*.

24 February 2021; resubmitted 23 July 2021
Accepted 1 October 2021
10.1126/science.abh2444

Science

Stem cells expand potency and alter tissue fitness by accumulating diverse epigenetic memories

Kevin Andrew Uy GonzalesLisa PolakIrina MatosMatthew T. TierneyAnita GolaEllen WongNicole R. InfarinatoMaria NikolovaShijing LuoSiqi LiuJesse S. S. NovakKenneth LayHilda Amalia PasolliElaine Fuchs

Science, 374 (6571), eabh2444. • DOI: 10.1126/science.abh2444

Stem cells remember

Tissue stem cells sense their surroundings, and this perception influences subsequent fate and function. Gonzales *et al*. observed that stem cells accumulate epigenetic memories of diverse environmental events (see the Perspective by Hoste). By wounding skin and monitoring the temporal steps involved in mobilizing stem cells of the hair follicle to repair the epidermis, the authors found that stem cells bear memories of their original niche, migration, encounters with inflammation, and adaptation to the new fate and tasks. During homeostasis, immigrant stem cells are functionally and transcriptionally analogous to native cells, but upon future assaults, they unleash discrete epigenetic memories to heighten physiological response and affect tissue fitness. —BAP

Science (ISSN) is published by the American Association for the Advancement of Science. 1200 New York Avenue NW, Washington, DC 20005. The title *Science* is a registered trademark of AAAS.